A Numerical Study of Low-Grazing-Angle Backscatter from Ocean-Like Impedance Surfaces with the Canonical Grid Method

Joel T. Johnson

***Abstract*— A numerical study of 14-GHz low-grazing-angle (LGA) backscattering from ocean-like surfaces described by a Pierson–Moskowitz spectrum is presented. Surfaces rough in one dimension are investigated with Monte Carlo simulations performed efficiently through use of the canonical grid expansion in an iterative method of moments. Backscattering cross sections are illustrated at angles from 81° to 89° from normal incidence under the impedance boundary condition (IBC) approximation with the efficiency of the numerical model enabling sufficiently large profiles (8192 λ) to be considered so that angular resolution problems can be avoided. Variations with surface spectrum low-frequency cutoff (ranging over spatial lengths from 175.5 m to 4.29 cm) at 3 m/s wind speed are investigated and initial assessments of the small perturbation method (SPM), composite surface theory, operator expansion method (OEM), small slope approximation (SSA), and curvature corrected SPM predictions are performed. Numerical results show an increase in horizontal (HH) backscatter returns as surface low-frequency content is increased while vertical (VV) returns remain relatively constant, as expected, but none of the approximate models considered are found to produce accurate predictions for the entire range of grazing angles. For the cases considered, HH scattering is always observed to be below VV, further demonstrating the importance of improved hydrodynamical models if "super-event" phenomena are to be modeled.**

***Index Terms*—Sea surface electromagnetic scattering.**

I. Introduction

RECENT improvements in experimental techniques [1]–[6] and hydrodynamical models [7]–[9] have sparked renewed interest in attempts to model near-grazing-angle backscattering from the ocean surface. However, since the accuracy of the standard electromagnetic approximations [10]–[13] as well as many recently proposed approximate models [14]–[21] in this region is not well understood, Monte Carlo approaches using numerical models for electromagnetic scattering from ocean-like surfaces have become the method of choice for obtaining insight into the scattering process. Previous numerical studies with ocean-like surfaces have been performed for incidence angles ranging from 0° to 70° [22]–[35], and have generally demonstrated the success of the composite surface model [13] in this angular region. Studies for greater than 70° incidence have been more limited [24], [25], [29], [30] due to the fact that use of a "tapered" wave incident field to avoid edge effects in finite-size surface simulations results in a loss of angular resolution in scattered fields as grazing incidence is approached. Angular resolution can be regained by using longer surface profiles in the simulation so that tapered wave spot sizes become larger on the surface, but the computational resources required increase as well so that previously no numerical results have involved surfaces larger than a few hundred electromagnetic wavelengths or grazing angles less than 5°–10°. Some recent studies have focused on deterministic feature-like targets and used a hybrid method [36], which analytically extends the target as a flat surface to infinity [37], [38] or else used periodic surfaces [26]–[28] so that plane wave incident fields without angular resolution problems can be used, but these techniques do not simultaneously model a full range of ocean length scales for microwave and higher frequencies. Thus, the angular region beyond 85° incidence for area extensive ocean-like surfaces has remained intractable numerically.

In this paper, a more efficient numerical approach is applied which enables much larger profiles to be considered so that backscattering for incidence angles greater than 85° can be accurately calculated. The method is based on use of a canonical grid expansion in an iterative point matching method of moments and has previously been applied to studies of Gaussian correlation function surface scattering at near grazing angles [32], propagation over the ocean [33], and ocean-like surface scattering at larger grazing angles [35]. Surface lengths of 8192λ (175.5 m at 14 GHz) with 65 536 unknowns are considered so that a 0.634° two-sided 3-dB beamwidth in the tapered wave incident field is obtained at 89° incidence. Only low-wind speeds are considered (3 m/s), but the 14-GHz frequency used results in a large wavenumber rms height ($k\sigma$) product of 14.25 for this case so that the surface is still very rough on an electromagnetic scale. In addition, the large surface size used allows the entire surface spectrum at this wind speed, which includes ocean-wave scales from the 8.2-m peak wavelength to the smallest Bragg wave at 1 cm to be modeled simultaneously. Simulations are performed using the impedance boundary condition (IBC) approximation to capture surface conductivity effects and initial comparisons with the first- and second-order small perturbation method (SPM) [11], composite surface theory [12], [13], small slope approximation

Manuscript received April 9, 1997; revised September 5, 1997. This work was sponsored by ONR contract N00014-9710541. Use of the IBM SP/2 at the Maui High-Performance Computing Center was sponsored by the Phillips Laboratory, Air Force Material Command under cooperative agreement F29601-93-2-0001.

The author is with the Department of Electrical Engineering and Electro-Science Laboratory, The Ohio State University, Columbus, OH 43210 USA.

Publisher Item Identifier S 0018-926X(98)01040-0.

(SSA) [14], operator expansion method (OEM) [16], and curvature corrected SPM predictions [39] are performed. In addition, variations in backscattered cross sections with spectrum low-frequency content are illustrated to investigate the physical basis of the composite surface theory and particular attention is given to the roll off in cross sections as grazing angles exceed 85°.

The next section briefly describes the ocean surface and approximate scattering models considered in this paper and Section III reviews issues associated with the numerical scattering model applied. Results are presented in Section IV and final conclusions are summarized in Section V.

II. Ocean Surface and Approximate Models

Surfaces to be used in the Monte Carlo simulation are modeled as realizations of a zero mean Gaussian stochastic process. The spectrum chosen for the ocean surface is a Pierson–Moskowitz spectrum as in [24]

$$\Psi(k') = \frac{\alpha}{4|k'|^3} \exp\left[-\left(\frac{\beta g^2}{|k'|^2 U^4}\right)\right] \tag{1}$$

where Ψ represents the ocean-spectrum amplitude in m^3, k' represents the spatial wavenumber of the ocean in rads/m and is defined to range over both positive and negative values, $\alpha = 0.008$, $\beta = 0.74$, $g = 9.81$ m/s^2, and U is the wind speed in m/s at a height of 19.5 m. Surface spectra used in the numerical simulations however will be set to zero outside of wavenumbers $k_{dl} < |k'| < k_{du}$ so that the effects of changing surface spectral content can be investigated. Note that the Pierson–Moskowitz spectrum does not include surface tension effects or recently proposed improved models for the capillary wave portion of the spectrum [40], but numerical and analytical model results will still be compared for exactly the same surfaces, allowing meaningful conclusions to be drawn regarding approximate model accuracy. Expressions for surface height and slope variances can be found in [24].

Numerically predicted backscattering cross sections will be compared with those of SPM with and without curvature corrections, composite surface theory, small slope approximation, and operator expansion method. Comparison of Monte Carlo SPM results with their analytically evaluated counterparts will be used to assess the influence of finite surface size and finite number of realizations on Monte Carlo predictions, as demonstrated in [41], and Monte Carlo OEM results will be obtained for the same set of surfaces as used with the canonical grid model. Expressions for one-dimensional (1-D) surface analytical theories with impedance surfaces were derived following [13], [14], [24], and [42]. Previous numerical studies of the composite surface model [35] at larger grazing angles suggest choice of the cutoff wavenumber parameter in the composite surface model as $k_d = k/2$ where k is the electromagnetic wavenumber corresponding to a two-wavelength spatial scale cutoff. Variations in this parameter will be considered in Section IV, however, in an attempt to produce improved composite theory predictions. The curvature correction to SPM cross sections, derived in [39] through consideration of a rough cylindrical surface, will also be applied with the radius of curvature of the cylindrical model R used as a parameter.

III. Numerical Model for Ocean Scattering

As discussed previously, numerical simulation of grazing angle backscattering from rough surfaces is complicated by use of a tapered Gaussian-beam incident field to eliminate edge effects in the study, which has the effect of reducing the angular resolution of obtained cross sections as discussed in [29]. An incident field of the form [43]

$$E_y = e^{i\overline{k}_i \cdot \overline{r}(1+W)} e^{-(x+z\,\tan\,\theta_i)^2/g^2} \tag{2}$$

where the y direction is perpendicular to the 1-D surface profile, which lies in the xz plane

$$\overline{k}_i = \hat{x}k_{xi} - \hat{z}k_{zi} = \frac{2\pi}{\lambda}(\hat{x}\,\sin\,\theta_i - \hat{z}\,\cos\,\theta_i) \tag{3}$$

g is a parameter which determines the spot size of the Gaussian beam on the surface, λ is the electromagnetic wavelength, and θ_i is the angle of incidence used in the simulations. W in the above equation is a phase correction to make the above Gaussian beam a solution of the wave equation to within the order of $1/(kg\,\cos\,\theta_i)^2$ and is unity to within the same order [43]. If W is approximated as unity, the plane wave spectrum $A(k_x)$ of the above incident field can be shown to be

$$A(k_x) = e^{-(k_x - k_{xi})^2 g^2/4} \tag{4}$$

demonstrating the expected inverse proportionality between spot size on the surface and beamwidth of the incident wave. Values of g necessary to provide a given beamwidth can be derived from (4). A determination of one half the two-sided 3-dB beamwidth is obtained from

$$(k_x - k_{xi})^2 g^2/4 = -\ln\,\frac{1}{\sqrt{2}} \tag{5}$$

$$|\,\sin\,\theta - \sin\,\theta_i| = \frac{0.589}{\pi g/\lambda} \tag{6}$$

where $\delta\theta = \theta - \theta_i$ is one half the two-sided 3-dB beamwidth. Using $\theta_i = 89°$ and $g = 2,048\lambda$, a beamwidth of 0.634° is obtained with (6), which should provide reasonable accuracy for backscattering predictions as will be shown in Section IV. An overall surface size of $L = 8,192\lambda$ ($g = L/4$) is used in the simulation so that incident fields are approximately 35 dB down at surface edges, as has been used previously in the literature [32], [43].

Use of a canonical grid expansion in an iterative point matching method of moments is described in more detail in [32], [33]. The method is based on performing required matrix multiplies in a conjugate gradient matrix equation solver by dividing individual rows of the matrix into "strong" and "weak" regions. Strong matrix elements are defined to be those within a specified distance of the testing point and are computed exactly, resulting in a banded matrix multiply. Weak matrix elements are those outside the specified distance and are expanded in a power series about zero-height deviation from the testing point (the canonical grid expansion). Multiplications of individual terms in the weak matrix power series take

a convolutional form so that they can be performed with the fast Fourier transform (FFT) in the frequency domain, resulting in an order $N \log N$ algorithm for weak matrix multiplies. Convergence of the canonical grid series has been examined in [33], where it is shown that the number of terms required is proportional to the $k\sigma$ times slope parameter, resulting in a highly efficient solution for surfaces that have relatively small slopes and/or heights in terms of a wavelength. The method is thus expected to be more suited to lower frequencies and wind speeds. Efficiency of the method for the surfaces considered will be discussed in Section IV.

Conjugate gradient solver efficiency was increased by using a second conjugate gradient solution of the zero-order canonical grid term matrix with zero-strong matrix bandwidth as the preconditioner. The "dense" nature of this preconditioner was found to provide a more rapid convergence in the full matrix equation than other banded matrix preconditioners. Note that conjugate gradient solution of the preconditioned equation is clearly an order $N \log N$ procedure since matrix multiplies are completely performed through use of the FFT. However, rapid convergence of the preconditioner solution is also desirable since its iterations must be performed within every iteration of the overall matrix solution. Thus, the preconditioner solution was also preconditioned through use of a quasi-physical optics solution, which was based on an FFT operation to represent the right-hand side (or incident field) in terms of its plane wave spectrum, a multiplication by $1 - R_h$ or $1 + R_v$ where R_h and R_v are the Fresnel reflection coefficients for individual plane waves to generate the physical optics incident plus reflected wave solution and an inverse FFT to return fields to the space domain. Since these operations are all linear, they can be represented in terms of a matrix operator, which is the preconditioner used for the preconditioner equation. Use of the quasi-physical optics solution was found to produce rapid convergence in the preconditioner conjugate gradient solver with dramatically improved efficiency in the overall matrix equation solution.

The numerical model applied models the dielectric constant of the ocean through use of the IBC approximation, $\hat{n} \times \overline{E} = \eta_1 \hat{n} \times \overline{J}_S$ where η_1 is the impedance of the sea water medium [44]. This approximation is reasonable since sea water is a fairly high-loss medium at microwave frequencies with a dielectric constant of approximately $38 + i40$ at K_u band [45]. Some indication of the accuracy of the IBC for this case was obtained through a comparison of perturbation theory predictions using the IBC with those that included the exact equations for the specified dielectric constant. Backscattering cross sections were found to be within 0.2 dB for this case even at near-grazing angles, where IBC accuracy is expected to decrease due to the high dielectric constant of the sea water medium. Similar results were obtained with the composite surface model, demonstrating that the IBC's accuracy extends beyond the small-surface rms height case where the SPM is valid.

Numerical results will be presented in terms of the normalized incoherent backscattering radar cross section $\sigma_{\alpha\alpha}$ in the plane of incidence, defined in terms of the ensemble average scattered field intensity as

$$\sigma_{\alpha\alpha}(\theta) = \lim_{R\to\infty} \frac{R\left\langle |E^s_{\alpha\alpha} - \langle E^s_{\alpha\alpha}\rangle|^2 \right\rangle}{L|E^{(i)}_\alpha|^2} \tag{7}$$

as in [24], where θ refers to the polar angle of observation, $\alpha = h, v$ refers to the polarization, $|E^{(i)}_\alpha|$ refers to the magnitude of the incident field on the surface profile, L to the length of the surface profile, and the $\langle\cdot\rangle$ notation above indicates an ensemble average over realizations of the surface stochastic process. Note that cross-polarized cross sections are not available from a 1-D surface model. The denominator of this expression is actually evaluated as $2\eta/\cos\theta_i$ times the total power incident upon the surface for the tapered beam, given by the integration of the normal component of the incident Poynting vector over the surface profile. With the above definitions, 1-D cross sections integrated over all scattering angles in the plane of incidence should yield $\cos\theta_i$.

Results to be presented were calculated with the IBM SP/2 400 node parallel computer at the Maui High-Performance Computing Center (MHPCC) [46]. The IBM SP/2 is a collection of 400 RS-6000 (based on a POWER2 CPU) work stations, capable of around 250 MFLOP operation individually, networked through a high-performance communication system to allow groups of nodes to operate in combination as a parallel processor. Software libraries are available at the center to implement interprocess communications using simple routine calls so that development of parallel codes is relatively efficient. The codes of this paper use the parallel virtual machine (PVM) message passing library [47], which is a public domain package for UNIX communications. Due to the implicitly parallel nature of a Monte Carlo simulation, parallelization of the code was effectively perfect with only simple process starting and monitoring routines requiring any interprocess communications.

IV. Results

Results were generated using surface spectrum low-frequency cutoff wavenumber k_{dl} values of 146.6 rad/m (corresponding to a spatial scale of two free-space electromagnetic wavelengths) and 0.036 rad/m 8192 free-space wavelengths) with corresponding $k\sigma$ products of 0.088 and 14.25 and total surface rms slopes s of 0.075 and 0.158, respectively. The high-frequency surface cutoff was held fixed at $k_{du} = 586$ rad/m (one-half free-space wavelength) to insure that the Bragg portion of the spectrum was adequately modeled. Strong matrix bandwidths in the canonical grid method as described in [32], [33], ranged from 64 points in the lowest rms height case to 512 points for the highest with a corresponding increase in the number of canonical grid terms required from 3 to 15, respectively. These parameters were determined through tests on several surface realizations as described in [33] and insure that canonical grid series Green's functions are accurate to within 0.1% for all points on the surface outside the bandwidth region. Sixty-four realizations were averaged for fields incident at 81°, 83°, 85°, 87°, and 89° and computational times for a single angle, polarization, and surface realization ranged from

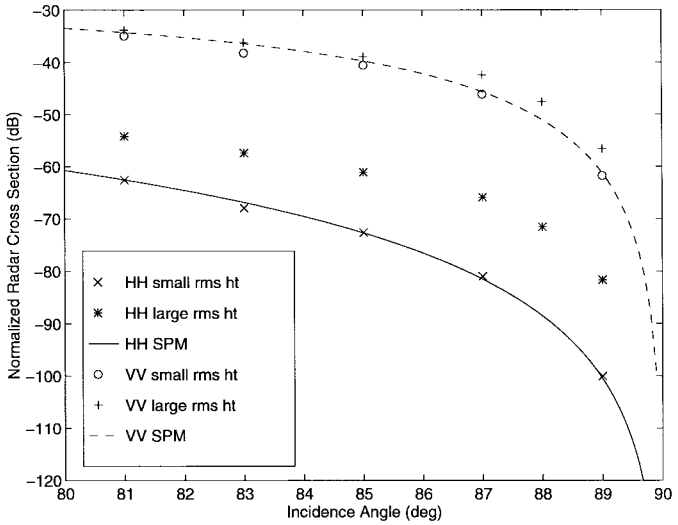

Fig. 1. Comparison of numerical and SPM backscattering predictions for small rms height case ($k_{dl} = 146.6$ rad/m, $k\sigma = 0.088$) and large rms height case ($k_{dl} = 0.036$ rad/m, $k\sigma = 14.25$).

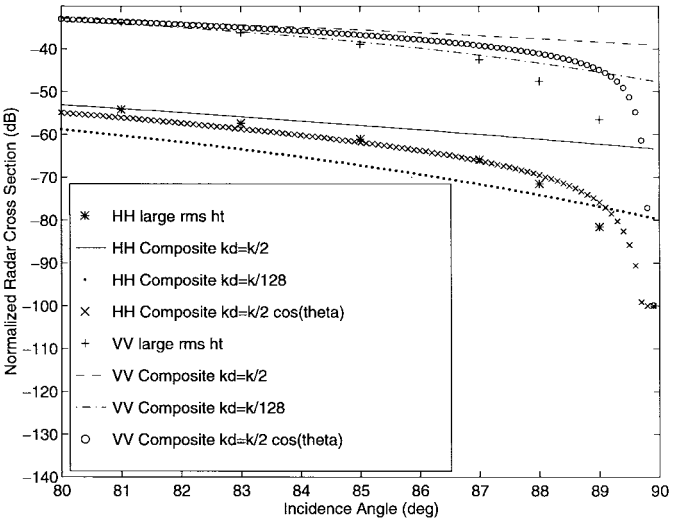

Fig. 2. Comparison of numerical and composite surface model backscattering predictions for large rms height case.

approximately 15 min on a single node of the SP/2 for the low-rms height cases to approximately 240 min in the high-rms height cases, illustrating the efficiency and expected rms height dependencies of the canonical grid approach. These computational times are very reasonable when the large number of unknowns in the simulation (65 536) is considered. Several numerical tests were performed varying the number of realizations, beam taper width, surface high-frequency content, surface sampling rate, and strong region bandwidth, and showed that the results presented should be accurate ensemble averages within approximately 2 dB for all cases considered.

Fig. 1 compares computed horizontal (HH) and vertical (VV) backscattered cross sections for the $k_{dl} = 146.6$ rad/m and $k_{dl} = 0.036$ rad/m cases. Also included in this plot are the corresponding SPM results. The excellent agreement between numerical and perturbation theory results (within 1 dB at all angles less than 87° and within 1.6 dB at 89°) in the low-rms height case clearly demonstrates that the numerical method can produce accurate predictions even up to 89° incidence. The small errors observed in these cross sections are caused by the finite number of realizations averaged and to the effects of the tapered beam. Monte Carlo SPM results were also computed and found to be in excellent agreement with numerical results (within 0.6 dB at all incidence angles), further demonstrating the accuracy of the SPM for the low rms height case. Numerical results for $k_{dl} = 0.036$ rad/m (where $k\sigma = 14.25$) clearly illustrate the effects of including surface low-frequency content. An additional point at 88° incidence was calculated for the large rms height case to provide more information on the roll off of cross sections beyond 87°. Horizontally polarized cross sections increase by up to 20 dB at 89° while vertically polarized cross sections show only a slight increase. Note also that HH cross sections decrease more slowly as grazing is approached than in the low-rms height case, clearly visible from the increasing difference between the two results near grazing incidence.

Fig. 2 compares numerical model results in the high-rms height case with those of the composite surface model. Three different choices for the cutoff wavenumber parameter in the composite surface model (which defines the upper limit to the low-frequency portion of the surface spectrum used in finding the "tilting" rms slope) are illustrated: $k_d = k/2$, $k/128$, and $\cos\,\theta_i k/2$. Fig. 2 clearly shows the standard choice $k_d = k/2$ to overpredict numerical results at smaller grazing angles, caused by the composite surface model's continued averaging over SPM results at larger grazing angles. The agreement obtained at larger grazing angles with $k_d = k/2$, however, gives an additional validation of the numerical method, since earlier numerical studies have shown good agreement with this choice at larger grazing angles. Choice of a much smaller value of $k_d = k/128$ greatly reduces the rms slope of the long wave portion of the spectrum so that smaller HH cross sections are obtained, but even with this decrease the composite surface theory again fails to predict the obtained angular dependence of the numerical results. An *ad hoc* choice of $k_d = \cos\,\theta_i k/2$ was made in an attempt to improve this behavior with some success as shown in the HH cross sections, but VV predictions remain inaccurate. Fig. 2 clearly shows that use of the composite surface model at near grazing angles requires an improved understanding of the k_d parameter in this angular region.

A Monte Carlo second-order SPM formulation was also derived for HH- and VV-polarized scattering from a 1-D impedance surface following the perfectly conducting HH formulation of [41]. However, second-order predictions, which resulted were found to exceed those of first order by more than 20 dB (even with the cancellation effects of σ_{22} and σ_{13} as defined in [41]) indicating a convergence problem in the SPM solution for this large $k\sigma = 14.25$ case. Comparisons with a mid-rms height case where $k_{dl} = 18.3$ rad/m and $k\sigma = 0.707$ showed second-order SPM predictions to work well, demonstrating that the method was implemented accurately so these comparisons show that higher order SPM formulations should

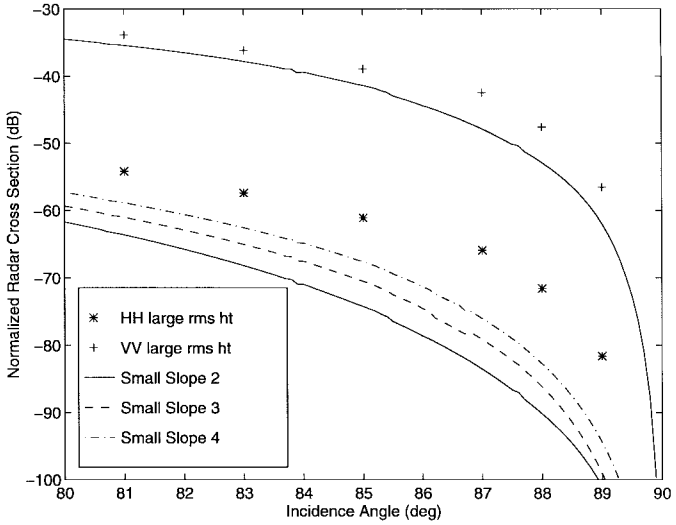

Fig. 3. Comparison of numerical and small slope approximation backscattering predictions for large rms height case.

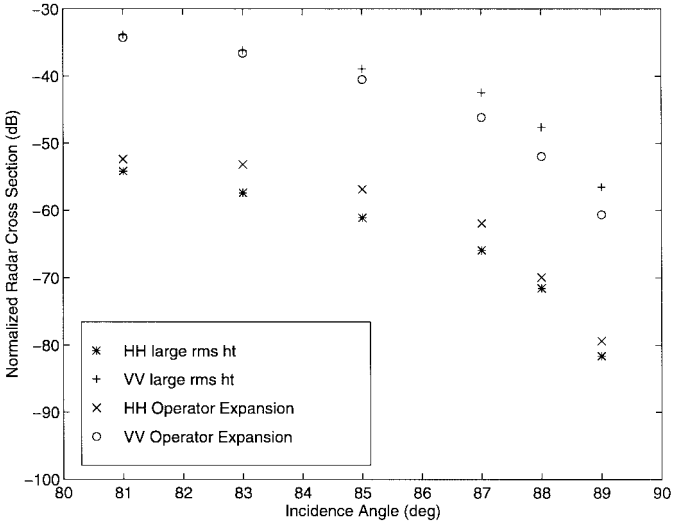

Fig. 4. Comparison of numerical- and operator-expansion method backscattering predictions for large rms height case.

be expected to have problems in the microwave frequency region where the $k\sigma$ product is usually very large.

Fig. 3 compares numerical cross sections in the large rms height case with predictions obtained from the small slope approximation for impedance surfaces. Both zeroth- and first-order terms were calculated for the SSA T-matrix (as defined in [42]) allowing computation (through numerical integration) of the SSA second-, third-, and fourth-order cross sections as defined in [42]. Results for HH cross sections show the second-order SSA prediction to be slightly smaller than the corresponding SPM result while higher order corrections gradually increase cross sections toward the canonical grid values. SSA predictions are seen to reproduce to some extent the roll off in cross sections as grazing angle is decreased, but substantial errors are still observed in the comparison to canonical grid results. It should be noted that [14] describes $s \ll \cos\theta$ as a condition of applicability of the SSA, where s is the surface rms slope, a condition that is clearly not met in this example. Further evidence of problems in the SSA is given by the fact that third- and fourth-order cross sections for VV results (not included in the plot) exceeded those of second order by more than 20 dB, as with higher order perturbation theory corrections. A more rapid failure of the SSA for VV polarization was also observed in [14].

Fig. 4 illustrates the comparison between canonical grid results and a method similar to the second-order symmetric operator expansion method of [16]. The OEM is an approach to scattering from a rough surface, which represents induced surface currents in terms of FFT operations on the incident field for a specified surface profile. A Monte Carlo simulation, performed for the same set of surfaces used in the canonical grid method, is thus required to obtain average scattering cross sections. As discussed in [16] and [33], the symmetric version of the OEM solves the same matrix equation as the canonical grid method, assuming that a zero strong matrix bandwidth is used. The order of the OEM depends on the number of weak matrix canonical grid series terms retained. Results presented in Fig. 4 are actually obtained from the canonical grid method with zero bandwidth and including only the zero and first-order CAG series terms, which corresponds to the $\hat{N}_0 + \hat{N}_2$ OEM solution. A direct OEM solution was not applied since a formulation for impedance surfaces was not readily available. Average cross section results show reasonable agreement in Fig. 4, but the errors that occur indicate problems with the operator expansion since the same set of surface realizations is used for both methods. Comparisons for individual surface realizations showed larger than 10-dB errors in some cases.

Fig. 5 compares numerical cross sections in the large rms height case with the curvature corrected SPM formulation of [39]. This formulation is based on the application of perturbation theory to a cylindrical surface with a specified radius of curvature R. The rms radius of curvature for the 3-m/s wind speed surfaces studied was calculated following [39] and found to be 32 cm using $k_d = k/2$, 11 cm using $k_d = k$. This model is seen to produce somewhat better agreement with numerical results than composite surface theory with a constant k_d, but again it is clear than the R parameter will require variation with grazing angle if the correct angular dependence is to be obtained. Note also that curvature corrections decrease VV cross sections below those predicted by planar perturbation theory, producing error at larger grazing angles.

Fig. 6 plots polarization ratios obtained numerically and from the SPM and composite models. Numerical polarization ratios in the low-rms height case are seen to agree well with perturbation theory, although somewhat larger errors are observed in this plot compared to Fig. 1 due to the increasing errors when HH and VV cross sections are combined. The slight average overestimation can be seen from Fig. 1 to be due to a slight underestimation of perturbation theory VV cross sections at large grazing angles and a slight overestimation of HH cross sections at small grazing angles, rather than a systematic error in cross sections themselves. Numerical polarization ratios obtained in the large rms height case are compared with those of composite surface theory (using $k_d = k/2$). It is interesting to note that composite surface theory

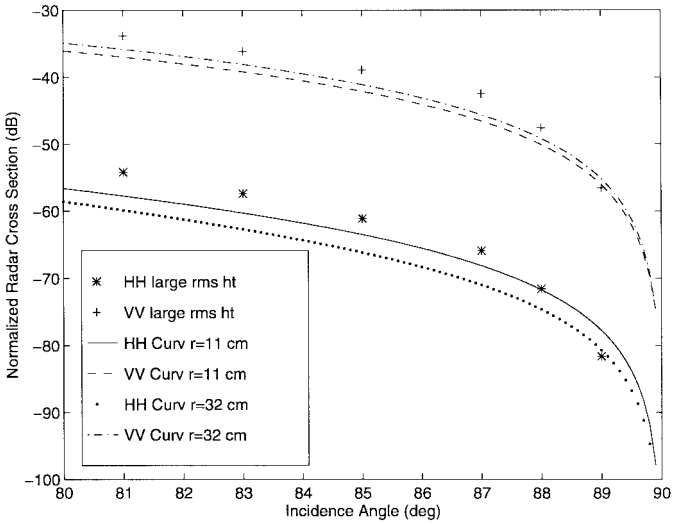

Fig. 5. Comparison of numerical and curvature corrected SPM backscattering predictions for large rms height case.

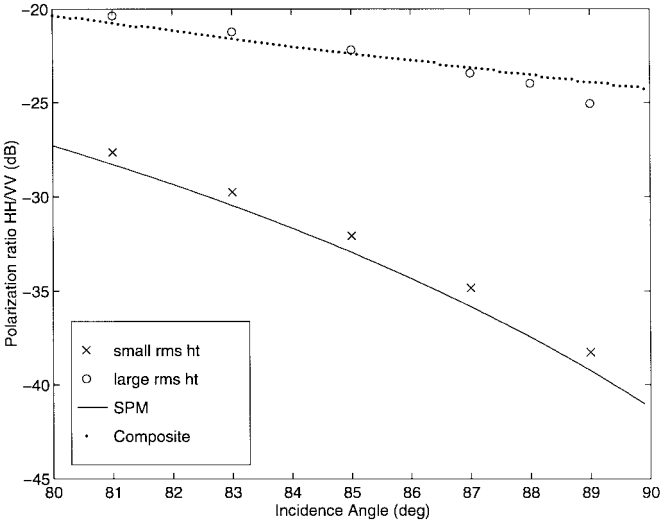

Fig. 6. Numerical, composite surface, and SPM polarization ratios.

continues to yield reasonable predictions of polarization ratios up to 88° even though it produces inaccurate predictions of HH and VV cross sections due to a cancellation of much of the cross-section angular dependency in the polarization ratio. Problems are still observed at 89°, however.

V. Conclusions

A numerical study of low-grazing-angle (LGA) backscattering for 1-D ocean like impedance surfaces has been performed. An efficient iterative point matching method of moments using a canonical grid expansion was used so that large surface profiles could be simulated to avoid angular resolution problems near-grazing incidence. Comparisons with perturbation theory in the small rms height limit show the numerical model to provide accurate predictions at up to 89° observation, and studies in a larger rms height case, corresponding to a full 3-m/s wind speed Pierson–Moskowitz ocean spectrum at 14 GHz, show problems in the standard analytical models as grazing incidence is approached. Both composite surface and curvature corrected SPM models were shown to require variations in their respective parameters with observation angle in order to reproduce the observed angular dependencies of numerical results and the second order SPM, small slope approximation, and operator expansion methods were also found to yield significant errors, showing that a better understanding of scattering physics in this region is needed if reliable analytical models are to be developed. Also, no cases where HH cross sections exceeded VV were observed in this study, giving further evidence of the importance of improved ocean-surface statistical models, which can contain wedge-like features [48]–[51] if "super event" behaviors (where HH cross sections exceed VV) are to be observed.

The results of this paper demonstrate the capability of the canonical grid method for studying ocean scattering at LGA's. Use of improved models for the ocean surface and its hydrodynamic evolution and comparisons with experimental measurements (in which sensors ideally would have similar angular resolutions to the incident fields of the numerical model) should allow further insight into the scattering physics of LGA sea clutter so that new analytical models can be developed. Scattering from two-dimensional surfaces, necessary for prediction of cross-polarized cross sections, has also been studied with the canonical grid approach at larger grazing angles [35], [52]–[54].

References

[1] P. H. Y. Lee, J. D. Barter, K. L. Beach, C. L. Hindman, B. M. Lake, H. Rungaldier, J. C. Shelton, A. B. Williams, R. Yee, and H. C. Yueh, "X band microwave backscattering from ocean waves," *J. Geophys. Res.*, vol. 100, no. C2, pp. 2591–2611, 1995.

[2] D. J. McLaughlin, N. Allan, E. M. Twarog, and D. B. Trizna, "High resolution polarimetric radar scattering measurements of low grazing angle sea clutter," *IEEE J. Oceanic Eng.*, vol. 20, no. 3, pp. 166–178, 1995.

[3] D. B. Trizna, J. P. Hansen, P. Hwang, and J. Wu, "Laboratory studies of radar sea spikes at low grazing angles," *J. Geophys. Res.*, vol. 96, no. 7, pp. 12529–12537, 1991.

[4] N. Ebuchi, H. Kawamura, and Y. Toba, "Physical processes of microwave backscattering from laboratory wind wave surfaces," *J. Geophys. Res.*, vol. 98, no. C8, pp. 14669–14681, 1993.

[5] A. D. Rozenberg, D. C. Quigley, and W. K. Melville, "Laboratory study of polarized scattering by surface waves at grazing incidence: Part I—Wind waves," *IEEE Trans. Geosci. Remote Sensing*, vol. 33, no. 4, pp. 1037–1046, 1995.

[6] M. A. Sletten and J. Wu, "Ultrawideband, polarimetric radar studies of breaking waves at low grazing angles," *Radio Sci.*, vol. 31, no. 1, pp. 181–192, 1996.

[7] R. Cointe and M. P. Tulin, "A theory of steady breakers," *J. Fluid Mech.*, vol. 276, pp. 1–20, 1994.

[8] M. S. Longuet-Higgins and R. P. Cleaver, "Crest instabilities of gravity waves Part I: The almost highest wave," *J. Fluid Mech.*, vol. 258, pp. 115–129, 1994.

[9] D. M. Milder, "The effect of truncation of surface wave Hamiltonians," *J. Fluid Mech.*, vol. 216, pp. 249–262, 1990.

[10] P. Beckmann and A. Spizzichino, *The Scattering of Electromagnetic Waves From Rough Surfaces*. New York: Pergamon, 1963.

[11] S. O. Rice, "Reflection of electromagnetic waves from slightly rough surfaces," *Commun. Pure Appl. Math.*, vol. 4, pp. 361–378, 1951.

[12] J. W. Wright, "A new model for sea clutter," *IEEE Trans. Antennas Propagat.*, vol. AP-16, pp. 217–223, 1968.

[13] G. R. Valenzuela, "Theories for the interaction of electromagnetic and oceanic waves: A review," *Boundary Layer Meteorol.*, vol. 13, pp. 61–85, 1978.

[14] A. G. Voronovich, *Wave Scattering from Rough Surfaces*. Berlin, Germany: Springer-Verlag, 1994.
[15] A. Ishimaru and J. S. Chen, "Scattering from very rough surfaces based on the modified second order Kirchhoff approximation with angular and propagation shadowing," *J. Acoust. Soc. Amer.*, vol. 88, pp. 1877–1888, 1990.
[16] D. M. Milder, "An improved formalism for wave scattering from rough surfaces," *J. Acoust. Soc. Amer.*, vol. 89, pp. 529–541, 1991.
[17] R. Dashen and D. Wurmser, "A new theory of scattering from a surface," *J. Math. Phys.*, vol. 32, pp. 971–985, 1991.
[18] E. Rodriguez and Y. Kim, "A unified pertubation expansion for surface scattering," *Radio Sci.*, vol. 27, pp. 79–93, 1992.
[19] A. K. Fung, Z. Li, and K. S. Chen, "Backscattering from a randomly rough dielectric interface," *IEEE Trans. Geosci. Remote Sensing*, vol. 30, pp. 356–369, 1992.
[20] R. E. Collin, "Full wave theories for rough surface scattering: An updated assessment," *Radio Sci.*, vol. 29, pp. 1237–1254, 1994.
[21] S. T. McDaniel, "A small-slope theory of rough surface scattering," *J. Acoust. Soc. Amer.*, vol. 95, pp. 1858–1864, 1994.
[22] C. Macaskill, and B. J. Kachoyan, "Numerical evaluation of the statistics of acoustic scattering from a rough surface," *J. Acoust. Soc. Amer.*, vol. 84, pp. 1826–1835, 1988.
[23] S. L. Durden, and J. F. Vesecky, "A numerical study of the separation wavenumber in the two scale scattering approximation," *IEEE Trans. Geosci. Remote Sensing*, vol. 28, pp. 271–272, 1990.
[24] E. I. Thorsos, "Acoustic scattering from Pierson–Moskowitz sea surfaces," *J. Acoust. Soc. Amer.*, vol. 88, pp. 335–349, 1990.
[25] C. L. Rino, T. L. Crystal, A. K. Koide, H. D. Ngo, and H. Guthart, "Numerical simulation of backscatter from linear and nonlinear ocean surface realizations," *Radio Sci.*, vol. 26, pp. 51–71, 1991.
[26] E. Rodriguez, Y. Kim, and S. L. Durden, "A numerical assessment of rough surface scattering theories: Horizontal polarization," *Radio Sci.*, vol. 27, pp. 497–513, 1992.
[27] Y. Kim, E. Rodriguez, and S. L. Durden, "A numerical assessment of rough surface scattering theories: Vertical polarization," *Radio Sci.*, vol. 27, pp. 515–527, 1992.
[28] R. Chen and J. C. West, "Analysis of scattering from rough surfaces at large incidence angles using a periodic-surface moment method," *IEEE Trans. Geosci. Remote Sensing*, vol. 33, pp. 1206–1213, 1995.
[29] C. L. Rino and H. D. Ngo, "Application of beam simulation to scattering at low grazing angles: Oceanlike surfaces," *Radio Sci.*, vol. 29, pp. 1381–1391, 1994.
[30] P. J. Kaczkowski and E. I. Thorsos, "Application of the operator expansion method to scattering from one-dimensional moderately rough Dirichlet random surfaces," *J. Acoust. Soc. Amer.*, vol. 96, pp. 957–968, 1994.
[31] D. A. Kapp and G. S. Brown, "A new numerical method for rough surface scattering calculations," *IEEE Trans. Antennas Propagat.*, vol. 44, pp. 711–721, 1996.
[32] L. Tsang, C. H. Chan, K. Pak, and H. Sangani, "Monte Carlo simulations of large scale problems of random rough surface scattering and applications to grazing incidence with the BMIA/canonical grid method," *IEEE Trans. Antennas Propagat.*, vol. 43, pp. 851–859, 1995.
[33] J. T. Johnson, "An extension of the canonical grid method for two-dimensional scattering problems," *IEEE Trans. Antennas Propagat.*, to be published.
[34] J. T. Johnson, R. T. Shin, J. Eidson, L. Tsang, and J. A. Kong, "A method of moments model for VHF propagation," *IEEE Trans. Antennas Propagat.*, vol. 45, pp. 115–125, Jan. 1997
[35] J. T. Johnson, R. T. Shin, J. A. Kong, L. Tsang, and K. Pak, "A numerical study of the composite surface model for ocean scattering," *IEEE Trans. Geosci. Remote Sensing*, to be published.
[36] W. D. Burnside, C. L. Yu, and R. J. Marhefka, "A technique to combine the geometrical theory of diffraction and the moment method," *IEEE Trans. Antennas Propagat.* vol. AP-23, pp. 551–558, 1975.
[37] J. C. West, J. M. Sturm, and M. A. Sletten, "Small grazing angle scattering from a breaking water wave: Demonstration of Brewster angle damping," in *IGARSS'96, Conf. Proc.*, Lincoln, NE, 1996, vol. IV, pp. 2207–2209.
[38] D. Holliday, L. L. Deraad, and G. J. St-Cyr, "Forward–backward: A new method for computing low grazing angle scattering," *IEEE Trans. Antennas Propagat.*, vol. 44, pp. 722–729, 1996.
[39] A. G. Voronovich, "On the theory of electromagnetic waves scattering from the sea surface at low grazing angles," *Radio Sci.*, vol. 31, pp. 1519–1531, 1996.
[40] J. R. Apel, "An improved model of the ocean surface wave vector spectrum and its effects on radar backscatter," *J. Geophys. Res.*, vol. 99, pp. 16 269–16 291, 1994.
[41] E. I. Thorsos and D. R. Jackson, "The validity of the perturbation approximation for rough surface scattering using a Gaussian roughness spectrum," *J. Acoust. Soc. Amer.*, vol. 86, pp. 261–277, 1989.
[42] S. L. Broschat and E. I. Thorsos, "An investigation of the small slope approximation for scattering from a rough surface: Part II—Numerical studies," *J. Acoust. Soc. Amer.*, vol. 101, pp. 2615–2625, 1997.
[43] E. I. Thorsos, "The validity of the Kirchhoff approximation for rough surface scattering using a Gaussian roughness spectrum," *J. Acoust. Soc. Amer.*, vol. 83, pp. 78–92, 1988.
[44] K. M. Mitzner, "An integral equation approach to scattering from a body of finite conductivity," *Radio Sci.*, vol. 2, pp. 1459–1470, 1967.
[45] L. A. Klein and C. T. Swift, "An improved model for the dielectric constant of sea water at microwave frequencies," *IEEE Trans. Antennas Propagat.*, vol. AP-25, pp. 104–111, 1977.
[46] "Maui high-performance computing center world wide web site," World Wide Web, http:www.mhpcc.edu, 1995.
[47] A. Geist, A. Beguelin, J. Dongarra, W. Jiang, R. Manchek, and V. Sunderam, "PVM 3 user's guide and reference manual," Oak Ridge Nat. Lab., Oak Ridge, TN, Rep. ORNL/TM-12187, 1994.
[48] L. B. Wetzel, "Sea clutter," in *Radar Handbook*, M. Skolnik, Ed., 2nd ed. New York: McGraw-Hill, 1990, ch. 13.
[49] ——, "On microwave scattering by breaking waves," in *Wave Dynamics and Radio Probing of the Sea Surface*, O. M. Phillips and K. Hasselmann, Eds. New York: Plenum, 1986.
[50] ——, "Electromagnetic scattering from the sea at low grazing angles," in *Surface Waves and Fluxes: Current Theory and Remote Sensing*, G. L. Geernaert and W. J. Plant, Eds. Norwell, MA: Reidel, 1990, ch. 13.
[51] D. R. Lyzenga, A. L. Maffett, and R. A. Shuchman, "The contribution of wedge scattering to to the radar cross section of the ocean," *IEEE Trans. Geosci. Remote Sensing*, vol. GRS-21, pp. 502–505, 1983.
[52] K. Pak, L. Tsang, C. H. Chan, and J. T. Johnson, "Backscattering enhancement of electromagnetic waves from two dimensional perfectly conducting random rough surfaces based on Monte Carlo simulations," *J. Opt. Soc. Amer.*, vol. 12, pp. 2491–2499, 1995.
[53] J. T. Johnson, L. Tsang, R. T. Shin, K. Pak, C. H. Chan, A. Ishimaru, and Y. Kuga, "Backscattering enhancement of electromagnetic waves from two dimensional perfectly conducting random rough surfaces: A comparison of Monte Carlo simulations with experimental data," *IEEE Trans. Antennas Propagat*, vol. 44, pp. 748–756, 1996.
[54] J. T. Johnson, R. T. Shin, J. A. Kong, L. Tsang, and K. Pak, "A numerical study of ocean polarimetric thermal emission," *IEEE Trans. Geosci. Remote Sensing*, to be published.

Joel T. Johnson (M'96) received the B.S. degree in electrical engineering from the Georgia Institute of Technology, Atlanta, in 1991 and the S.M. and Ph.D. degrees from the Massachusetts Institute of Technology, Cambridge, in 1993 and 1996, respectively.

He is currently an Assistant Professor in the Department of Electrical Engineering and ElectroScience Laboratory of The Ohio State University, Columbus. His research interests are in the areas of microwave remote sensing, propagation, and electromagnetic wave theory.

Dr. Johnson is a member of Tau Beta Pi, Eta Kappa Nu, and Phi Kappa Phi. He held a National Science Foundation Graduate Fellowship from 1991 to 1995, received the 1993 Best Paper Award from the IEEE Geoscience and Remote Sensing Society, and has been named a 1997 Office of Naval Research Young Investigator and National Science Foundation Career Award recipient.